

Parametric Analysis of Impingement Gaps on Hot Steel Plate Cooling by Water Jet

¹Onah T.O., ²Odukwe A.O. and ³Egbuna S.O.

¹Department of Mechanical and Production Engineering, Enugu State University of Science and Technology Enugu, Enugu Nigeria.

²Department of Mechanical Engineering, University of Nigeria Nsukka, Enugu Nigeria.

³Department of Chemical Engineering, Enugu State University of Science and Technology Enugu, Nigeria.

Email address: Okechukwutm@yahoo.com.

ABSTRACT

Parametric experimental studies were carried out in order to investigate and analyze effect of impingement gaps on a hot steel plate. An impingement cooling system was designed for this goal. Analysis were carried out to determine the Convective Heat Transfer Coefficient, h , under multiple water jet of impingement gaps with 30 number holes. Tests were run with water cooling distributions of pipe diameter, D , of 20mm, 25mm, 32mm and 45mm, and impingement gaps, H , of 40mm, 50mm, 60mm and 70mm respectively. The hot steel plate is a carbon-steel of 230mm by 120mm thickness, instrumented with a three chromel-Alumel K-type thermocouple from the bottom of the plate till nearly 1mm to the top surface of the plate. The plate was heated in a furnace at temperature of 920°C and quickly transported to cooling area via bolt and screw motorized conveyor. Cooling was done from surface temperatures range of 430°C to 550°C to a controlled accelerated cooling temperature of 200°C. Results obtained were reduced and analyzed by conduction, boiling and convection heat transfer modelling. This accounted for transient temperature-time cooling by analyzing for zero temperature using Visual Basic Heat Transfer (VBHT) model development across the hot steel plate thickness. Based on the results obtained for $T_0 = \frac{T_s K - \Delta x (h T_{\infty} - 2257000V)}{K - h \Delta x}$, optimum cooling occurred at small pipe diameter, D , of 20mm at impingement gap, H , of 70mm and big pipe diameter, D , of 45mm at impingement gap, H , of 40mm at controlled cooling temperature of 300°C. This parametric study showed that with the small pipe diameter, the rate of cooling occurred at high impingement gap, but with big pipe diameter the rate of cooling is better achieved with small diameter pipe. This could be as a result of streamwise velocity, that water jet velocity for planar jet does not decrease, whereas water jet velocity in parallel flow zone of circular jets decreases.

Keywords: Impingement cooling system, impingement gaps, thermocouples, pipe diameters, hot steel plate, temperatures and transient heat transfer.

INTRODUCTION

Steel companies that aim to produce steel plates of various qualities and thicknesses invariably start by re-heating steel slabs from the continuous casting plant to rolling temperatures of about

900°C. This is then followed by passing the re-heated slabs through a number of rolling-stands. Subsequently, the rolled plates are cooled, on lines, on the run-out table [1, 2].

Water impinging as a jet onto a solid surface occurs in five different configurations, i.e. free-surface, plunging, submerged, confined, and wall jets [3]. However, on a run out table in a hot rolling mill, only free-surface and plunging jets are observed as shown in (fig.1).

In free- surface impingement, the liquid jet impinges on a surface on which there is not a pool of liquid covering the

surface. However, in the plunging jet, the water impinges on preexisting water that has accumulated on the surface of the steel. The water depth on the surface is less than the nozzle to surface spacing. Plunging jets are commonly encountered in strip and plate mills [5]. Intuitively, an existing water layer may decrease force convective effects of jet impingement and consequently, cooling efficiency of jets. The current study concentrates on free surface jet impingement cooling via a water pump.



Fig. 1.: Schematic diagram of water impinging as a jet onto a surface (a) the free surface and (b) plunging jets.

In a free-surface impingement type cooling, upon impinging, the liquid changes direction to transverse along the surface and generate evaporation and boiling. Nozzle to surface spacing (H_n) can influence the velocity and the size of the water jet before impinging on the surface. The continuity equation of volume flow rate is used to calculate the jet impingement velocity V_j [6].

Hernandez (2011), developed a heat transfer model for planar water jet cooling on the run-out table. Similar to previous studies, the size of the cooling zone was held constant i.e., independent of surface temperature. To find heat flux in either the impingement or the parallel flow zone, the macrolayer evaporation mechanism was adopted for contribution of nucleate boiling in the transition boiling regime

Generally, many researchers use initial and final temperatures of the strip/plate and apply a fitting procedure to find heat

transfer coefficient [7, 8, 9]. However, these results are mill dependent, as they do not accurately predict the temperature of steel strip on another run-out table with different operating parameters, since the fundamental heat transfer model for the steel strip cooled by planar jet and coiled is above 600°C . Moreover, the emphasis of almost all heat transfer model is for jet impingement cooling for temperature higher than 600°C . However, for the production of advanced Thermo Mechanical- Controlled Process (TMCP) steel accelerated cooling needs to be extended to lower temperatures lower than 600°C , where evaporation cooling, transition and nucleate cooling are dominant.

Thus, this work tries to lower the cooling temperature to 200°C from exposed (initial) temperature of 550°C , lower than 600°C in the literatures, with different pipe diameters, D , of 20mm and 45mm, and impingement gaps, D , of 40mm and 70mm.

MATERIALS AND METHODS

Experimental Set -Up For Pilot Scale Plant Run Out Table

In this research, a pilot scale run out table (ROT) facility was designed and

constructed in Mechanical and Metallurgical Engineering Foundry Laboratory (MMEFL), ESUT. A schematic diagram of the run-out table is shown fig.2.

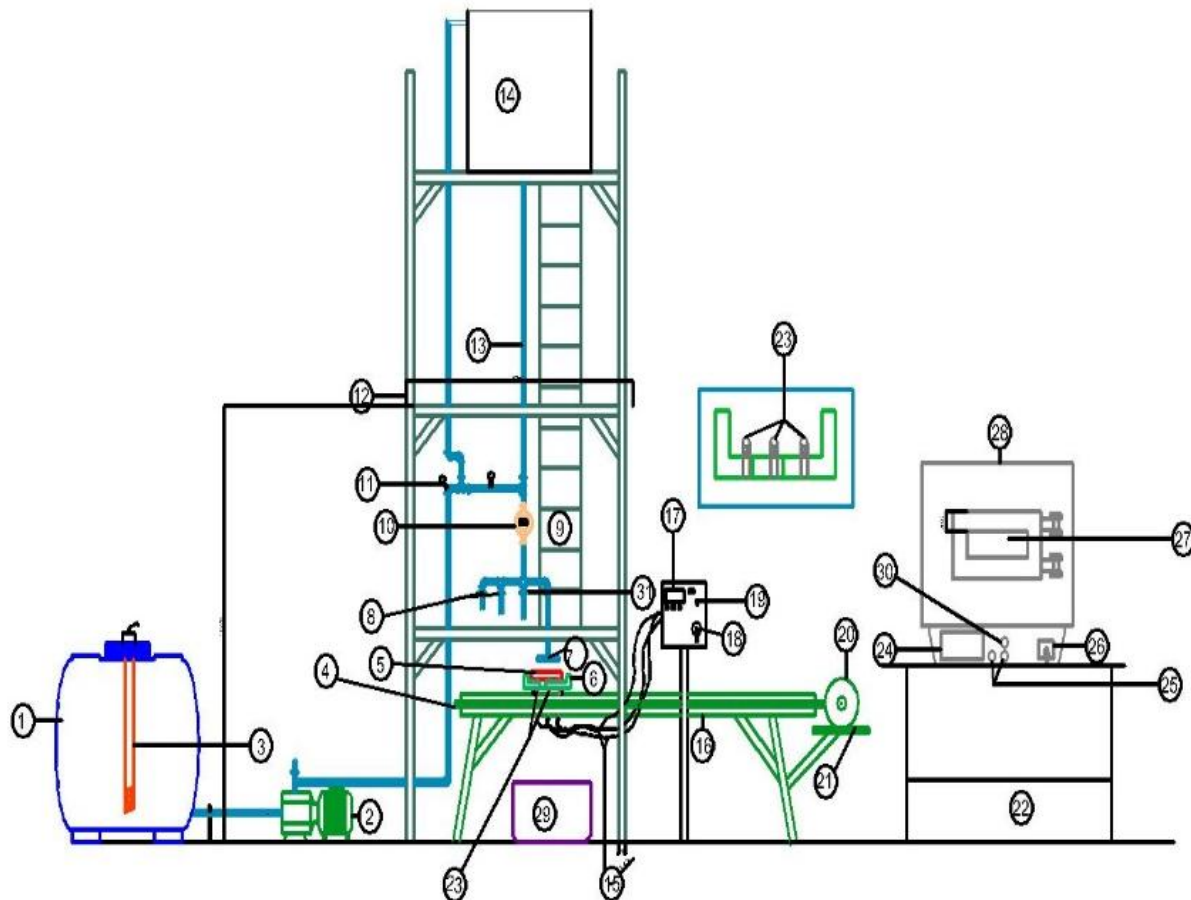


Fig.2: Schematic diagram of a pilot run out table

28.Electric furnace, 29.Water collector, 30.Pilot light Header.

- 1.Water tank, 2. Electric pump,3.Heater,
- 4.Conveyor screw, 5.Work piece,
- 6.Work piece bed, 7.Impingement nozzle,
- 8.Ball gauge socket, 9.Ladder,
- 10.Flow meter, 11.Pressure meter,
- 12.Tower, 13.PVC pipe, 14.Reservoir,
- 15.Thermocouple wire, 16.Motorized Screw conveyor,
- 17.Thermocouple control panel, 18.Regulator,
- 19.Lock, 20.Electric motor, 21.Electric motor support,
- 22.Furnace support, 23.Thermocouple,
- 24.Furnace indicator, 25.Furnace switch,
- 26.Furnace regulator, 27.Furnace door,

The facility has been designed to simulate industrial cooling condition for run-out table cooling of stationary plates in hot strip and plate mills [10]. It enables heat transfer to be studied during cooling of stationary plates. The heating was provided by an electric furnace where a steel plate was heated up to a temperature of 920°C in Metallurgical and Material Laboratory ESUT Enugu, Nigeria. A motorized ASYNCHROME ROTOR gear powered conveyor drive system of 750w of 1500rpm was used to operate a gear of 1:24 by ratio with 50HZ.Under an AC. of

240volts, the steel plates were transported from the furnace to the cooling tower for the stationary experiments.

The cooling system featured a closed water loop where 0.945m³ of water was circulated throughout the experiment through the cooling jet nozzles. Surface temperatures, water temperatures, impingement heights or nozzle-to-surface spacing (impingement gap) and flow rates were controlled. An ATLAS (ATP 60) water pump that provided total water flow rates of 0.001m³/sec was employed. It pumped water to the impingement plate from the water tank below to the target plate through the flow meter, nozzle header via impingement jet nozzle to the

Experimental procedure

After the required temperature of 920°C was reached in the electric furnace, the workpiece was removed and kept on the motorized screwed conveyor that transported the plate towards the cooling jet impingement target. For the experiment, the center of the plate was positioned under the jet nozzle, and the water flow from tank was started. The water header was positioned for different flow of water using different water pipe diameters and heights. The pressure gauge and flow meter were also opened to read the values of pressure and flow rate with stop watch. However, the initial surface temperatures of the plate (Ti) at

Experimental sequence

Experiments were carried out at several water flow rates via flow meter to target heated plates. The procedures were sequentially explained below: The water supply to the flow line via flow meter to the hot plate through the header and at various pipe diameter through jet nozzle was turned on. The 9000w electric heater was turned to vary the water temperature. Thereafter, the readings of the parameters under investigations were read.

Readings were monitored until nearly steady state isothermal condition was achieved i.e. T_1 , T_2 , T_3 were within 0.5% of each other with the average surface

hot plate. An electric heater of 9000w of 330volts was situated in the tank and was used to adjust the temperature of water between 10°C to 70°C. The water temperature readings were taken with a mercury in bulb thermometer.

In this work, planar (water) nozzle was used. The cross section was 12x 12 mm size, with 0.8mm diameter drill of 30 number holes. A control panel was to read the surface temperatures of steel before and after the impingement. It has a red icon button that controlled and recorded the temperatures with digital read out on a steel cased panel.

the onset of water impingement cooling varied from 450 to 550°C. Temperature data of various thermocouple locations were collected when the surface temperature was within $\pm 3^\circ\text{C}$ of the three thermocouples. Then, the average initial or surface temperature was recorded. When the controlled impingement cooling reached 200°C, 180°C, 160°C and 300°C, 280°C and 260°C respectively, the flow was controlled using stop watch. The evaporated water was obtained, by subtracting volume of water collected from volume of water used, with flow meter and measuring cylinder.

temperature of $\pm 3^\circ\text{C}$. Thereafter, final reading for particular flow rate of water say, Q_1 of diameter, D , of 20mm with impingement gap, H , of 40mm were recorded. Then another three sets of experiments of pipe diameters, D , of 25mm, 32mm, 45mm diameters and impingement gaps, H , of 40mm, 60mm and 70mm each for different controlled temperature cooling of 160 to 200°C and 260 to 300°C were recorded. After each flow of impingement water jet cooling, D and H , were repeated as above.

RESULTS AND DISCUSSION

Heat transfer model

Transient state temperature development across the workpiece thickness of 120mm.

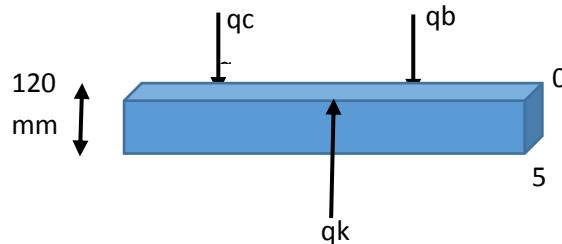


Fig. 3: Sketch of energy balance

The transient state temperature development across the workpiece of 120mm, was evaluated as shown in fig.3, where q_k is conductive heat transfer, q_c is convective heat transfer and q_b is boiling heat transfer.

Boundary condition

The boundary conditions were applied at the top (surface of water jet impingement) and the bottom surfaces.

At the top surface; the boundary condition was solved using the energy balance of heat by conduction to be equal to heat by convection and that by boiling:

$$q_k = q_c + q_b \quad (1)$$

Where;

$q_k = -k \frac{\partial T}{\partial x} x_0$ = conductive heat transfer(kJ)

$q_c = h(T_0 - T_\infty)$ = convective heat transfer kJ, and

$q_b = mh_{fg}$ = heat out flow due to evaporation of cooling water (KJ).

Thus,

$$-k \frac{\partial T}{\partial x} = h(T_0 - T_\infty) + mh_{fg} \quad (2)$$

Where;

k = thermal conductivity of the fluid (water) (w/m,k)

∂T = change in temperature(°C)

∂x = division across the thickness of the workpiece in (mm)

h = coefficient of convective heat transfer in (w/m²k)

$(T_0 - T_\infty)$ =difference in zero surface temperature and temperature of the immediate

environment of the test plate (°C)

m = mass of water in (kg)

mh_{fg} = latent heat of vaporization of saturated water in (kJ/kg)

One Dimensional Mesh For Finite Difference Treatment of Temperature Development

Analysis was done by transient-state discretization of temperature across the workpiece for 1 -D heat treatment on the workpiece. At the bottom surface, the heat was assumed to be constant. Thus, the temperature at all points was the same

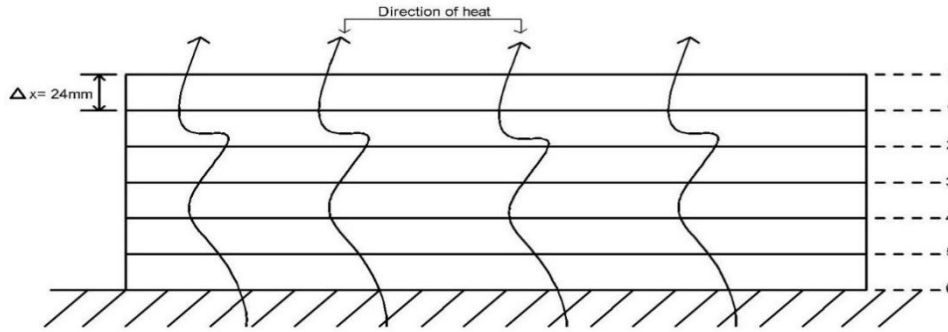


Fig. 4-Dimensional Mesh For Finite Difference Treatment of Temperature Development

The condition was approximated to an adiabatic bottom face (i.e. no heat lose to the workpiece supporting structure). Using Taylor series expansion allowed T_o , (Bangalore, 2014)

$$T_1 = T_o + \left(\frac{\partial T}{\partial x}\right)_o \Delta x + \frac{\partial^2 T}{\partial x^2} \frac{(\Delta x)^2}{2!} + \dots \quad (3)$$

$$\therefore \left(\frac{\partial T}{\partial x}\right)_o \Delta x = (T_1 - T_o) - \frac{\partial^2 T}{\partial x^2} \frac{(\Delta x)^2}{2!} - \dots \quad (4)$$

120mm

$$\text{Or } \left(\frac{\partial T}{\partial x}\right)_o \triangleq \frac{T_1 - T_o}{\Delta x} \quad (5)$$

Substituting equations (5) into (1), gave equation (6) as

$$q_k = -k(T_1 - T_o)/\Delta x = q_c + q_b$$

(6)

For $q_k = q_c + q_b$, then

$$-k \left\{ \frac{T_1 - T_o}{\Delta x} \right\} = h(T_o - T_\infty) + q_b$$

$$-k\{T_1 - T_o\} = h\Delta x (T_o - T_\infty) + \Delta x q_b$$

$$T_1 - T_o = -\frac{h}{k} \Delta x (T_o - T_\infty) - \frac{\Delta x}{k} q_b$$

$$\therefore T_o = T_1 + \frac{h}{k} \Delta x (T_o - T_\infty) + \frac{\Delta x}{k} q_b \quad (7)$$

Solving for real T_o ,

$$T_o = T_1 + \frac{h\Delta x}{k} T_o - \frac{h\Delta x}{k} T_\infty + \frac{\Delta x q_b}{k}$$

$$\text{and } T_o - \frac{h\Delta x}{k} T_o = T_1 - \frac{h\Delta x}{k} T_\infty + \frac{\Delta x q_b}{k}$$

$$\therefore T_o = \frac{k}{k - h\Delta x} \left\{ \frac{T_1 k - h\Delta x T_\infty}{k} \right\} + \frac{k}{k - h\Delta x} \left\{ \frac{\Delta x q_b}{k} \right\}$$

$$T_o = \frac{T_1 K - h\Delta x T_\infty}{K - h\Delta x} + \frac{\Delta x q_b}{k - h\Delta x} \quad (8)$$

$$T_o = \frac{T_1 K - h \Delta x T_{\infty} + \Delta x q_b}{K - h \Delta x} \tag{9}$$

Thus,

$$T_o = \frac{T_1 K - \Delta x (h T_{\infty} - q_b)}{K - h \Delta x} \tag{10}$$

$$T_o = \frac{T_2 K - \Delta x (h T_{\infty} - m h_{fg})}{K - h \Delta x} \tag{11}$$

$$T_o = \frac{T_2 K - \Delta x (h T_{\infty} - \rho V h_{fg})}{K - h \Delta x} \tag{12}$$

For $q_b = m h_{fg}$,

$$\text{Then, } q_b = 1000 \times V \times 2257 = 2257000 V \text{ kJ/m}^3 \tag{13}$$

Equation 12 gives equation 14 as,

$$T_o = \frac{T_2 K - \Delta x (h T_{\infty} - 2257000 V)}{K - h \Delta x} \tag{14}$$

Where T_o = surface zero temperature ($^{\circ}\text{C}$),

Convection model calculations

The value of h was estimated from Lui and Wang, (2014)

$$Nu = \frac{hD}{k} = \sqrt{2} Re^{\frac{1}{2}} * Pr^{\frac{1}{4}} * \left(\frac{k_v}{k_l}\right)^{\frac{1}{2}} * \left(\frac{\Delta T_{Sub}}{\Delta T_{Sat}}\right)^{\frac{1}{2}} \tag{15}$$

Where Nu is Nusselt Number, h is convective heat transfer coefficient ($\text{W/m}^2\text{k}$), k is thermal conductivity of steel (W/mk), D is the nozzle jet diameter (mm), Re is Reynolds Number, k_v and k_l are thermal conductivities of vapour and liquid ($\text{W/m}^{\circ}\text{C}$), respectively. ΔT_{sat} is the surface superheat which is the difference between the surface temperature and saturation temperature (boiling temperature of water). In the above equations ΔT_{sub} which is called subcooling was the difference between liquid temperature and saturation temperature.

At the end of the experimental run, during which the total amount of water impinged has been estimated and the non-evaporated was also estimated, the evaporated may be estimated as the

difference, and an average over time computed and used to calculate the quantity of mass transfer during the poll boiling or evaporation.

Calculation for the ratio of thermal conductivities of vapour and liquid

The thermal conductivity ratio of vapour and liquid is calculated from equation 16,

$$\left(\frac{k_v}{k_l}\right)^{\frac{1}{2}} \tag{16}$$

Where K_v and K_l are thermal conductivities of vapour and liquid at various temperatures respectively

$$\left(\frac{k_v}{k_l}\right)^{\frac{1}{2}} \text{ at } 200^{\circ}\text{C} = \left(\frac{0.0401}{0.663}\right)^{1/2} \tag{17}$$

Thus;

$$\left(\frac{k_v}{k_l}\right)^{\frac{1}{2}} \text{ at } 200^{\circ}\text{C} = (0.0605)^{1/2} \tag{18}$$

Calculation for Prandtl Number (Pr)

The Prandtl Number Pr was calculated from equation 19 as;

$$Pr = \frac{C_p \mu}{k} \text{ (Sergners and$$

Watson, 2015) (19)

Where C_p is the specific heat capacity of the liquid (water) (J/kg.K) = 4500 J/kg.K.

μ is the dynamic viscosity of liquid (water) (kg/m.s) = 0.122×10^{-3} kg/m.s,

$$\text{Thus, } Pr = \frac{4500 \times 0.122 \times 10^{-3}}{0.663} = 0.910 \text{ at } 200^\circ\text{C} \quad (20)$$

k is the thermal conductivity of liquid (water) = 0.663 w/m.k

Calculation for Reynolds Number (Re)

The values of Reynolds Numbers was obtained from equation (21),

$$Re =$$

$$\frac{\rho V D}{\mu} = \frac{v_{jet} D}{\nu} \text{ (Theodora L. et al., 2011)}$$

(21)

Where $\rho_{\text{liquid(water)}}$ = 1000 kg/m³ is the density of water.

V_{jet} is the velocity of water jet from the calculated flow rate using $\frac{Q_n}{n}$ for

n number of holes,
where ;

$$\text{But } V_j = \frac{Q_{jet}}{A} \quad (22)$$

$$Q_{jet} = \frac{Q_{flow \text{ rate}}}{30} \quad (23)$$

$$A = \frac{\pi D^2}{4} = \frac{3.142 \times 0.0008^2}{4} = 5.027 \times 10^{-7} \text{ m}^2 \quad (24)$$

$$\text{Also } V_j = \frac{Q_{jet}}{A} = \frac{\frac{Q_{flow \text{ rate}}}{30}}{\frac{\pi D^2}{4}} = \frac{4Q}{30 \times \pi \times 0.0008^2} = \frac{4Q}{0.00006033} \text{ m/s} \quad (25)$$

For D_{jet} = 0.0008 m ; ν = 0.573×10^{-6} m/s

Thus;

$$Re = \frac{\left(\frac{4Q}{0.00006033}\right) \times 0.0008}{0.573 \times 10^{-6}} = \frac{\left(\frac{4Q}{0.00006033}\right) \times 0.0008}{0.573 \times 10^{-6}} = \frac{53.042Q}{0.573 \times 10^{-6}} \quad (26)$$

$$Re = 92.57Q \times 10^6,$$

After which the values of Re were found ,where Q is calculated flow rates from experimental run.

Calculation for Nusselt Number (Nu)
The value of Nusselt Number was also calculated from equation 15, as shown

$$Nu = \sqrt{2} Re^{\frac{1}{2}} * Pr^{\frac{1}{6}} * \left(\frac{kv}{kL}\right)^{\frac{1}{2}} * \left(\frac{\Delta T_{Sub}}{\Delta T_{Sat}}\right)^{\frac{1}{2}}$$

Then substituting equations 18, 20 and 26 into 15, yields 28

$$Nu = \sqrt{2} (0.0605)^{1/2} * (0.910)^{1/6} * 92.57Q \times 10^6 * \left(\frac{\Delta T_{Sub}}{\Delta T_{Sat}}\right)^{\frac{1}{2}} \quad (27)$$

$$Nu = 31.702 * Q \times 10^6 \left(\frac{\Delta T_{Sub}}{\Delta T_{Sat}}\right)^{1/2}, \quad (28)$$

Then, values of Nusselt Number were found.

Calculation for Convective Heat Transfer Coefficient h.

$$\text{From } Nu = \frac{hD_{jet}}{k} \quad (\text{Theodora L. et al., 2011}) \quad (29)$$

Where;
h = convective heat transfer coefficient (w/m².k)

D^{jet} = diameter of impingement nozzle (m)
K = thermal conductivity of steel = 60.5 (w/m,k)

$$\text{Thus } h = \frac{KNu}{D_{jet}} \quad (30)$$

Substituting equation 28 into 30 gives

$$h = \frac{60.5 * 30.717 * Q * 10^6 * \left(\frac{\Delta T_{Sub}}{\Delta T_{Sat}}\right)_i^{\frac{1}{2}}}{D_{jet}} = \frac{0.0605 * 30.717 * Q * 10^6 * \left(\frac{\Delta T_{Sub}}{\Delta T_{Sat}}\right)_i^{\frac{1}{2}}}{0.0008} \quad (31)$$

$$h = 2322.97 * Q * 10^6 * \left(\frac{\Delta T_{Sub}}{\Delta T_{Sat}}\right)_i^{\frac{1}{2}} \quad (32)$$

From which the values of h were found.

From equations 14,18,20, 26, 28 and 32 respectively, tables 1 and 2 were simulated.

Table 1: Simulated values for Prandtl Number, Nusselt Number, Reynolds Number, Convective Heat Transfer Coefficient h, Flow Rate and Surface Temperature T_s for D=20mm, H=70mm, and D_{jet}=0.0008mm

Prandtl Pr. $Pr = \frac{C_p \mu}{k}$	$\left(\frac{k_v}{k_L}\right)^{\frac{1}{2}}$	$\left(\frac{\Delta T_{Sub}}{\Delta T_{Sat}}\right)_i$	Reynolds Re. $Re = 92.57Q \times 10^6$	Nusselt Nu. $Nu = 31.702 * Q$	Con.heatcoeff., h.(w/m ² k) $h = 2322.97 * Q * 10^6 * \left(\frac{\Delta T_{Sub}}{\Delta T_{Sat}}\right)_i^{\frac{1}{2}}$	Q * 10 ⁶ m/s	$T_s = \frac{T_c K - \Delta x (h T_c - 2257)}{K - h \Delta x}$
0.91	0.245	0.661	811.838	183.975	13480.8	8.77	228.638
0.947	0.239	0.621	825.724	175.727	12876.45	8.92	223.411
0.983	0.232	0.581	1080.292	215.096	15761.26	11.67	242.071
1.03	0.226	0.547	884.043	165.903	12156.61	9.55	212.726
1.09	0.220	0.512	707.512	124.225	9102.64	7.643	167.171
0.902	0.356	0.855	365.373	107.023	7842.178	3.947	134.269
0.878	0.339	0.821	480.901	135.243	9909.97	5.195	181.912
0.854	0.322	0.787	740.56	199.652	14629.54	8	233.421
0.843	0.303	0.769	875.712	230.739	16907.47	9.46	247.531
0.832	0.286	0.740	660.949	167.649	12284.53	7.14	213.868

Table 2: Simulated values for Prandtl Number, Nusselt Number, Reynolds Number, Convective Heat Transfer Coefficient h, Flow Rate and Surface Temperature T_o for D=45mm, H=40mm, and D_{jet}=0.0008mm

Prandtl Pr. $Pr = \frac{Cp\mu}{k}$	$\left(\frac{k_v}{k_L}\right)^{\frac{1}{2}}$	$\left(\frac{\Delta T_{Sub}}{\Delta T_{Sat}}\right)_i$	Reynolds Re. $Re = 92.57Q \times 10^6$	Nusselt Nu. $Nu = 31.702 \cdot h = 2322.97 \cdot Q \cdot 10^6 \left(\frac{\Delta T_{max}}{\Delta T_{min}}\right)^{\frac{1}{4}}$	Con.heat.coeff.,h. (w/m ² k)	$Q \cdot 10^3$ m/s	$T_o = \frac{T_s K - \Delta x (h T_m - 2257)}{K - h \Delta x}$
0.91	0.2459	0.6	799.897	164.36	12043.67	8.641	203.233
0.947	0.239	0.578	1295.98	256.57	18800.46	14	253.869
0.983	0.2326	0.553	2758.586	523.34	38348.02	29.8	290.421
1.03	0.2264	0.510	1712.545	299.16	21921.61	18.5	264.766
1.09	0.2206	0.466	1248.769	199.34	14607.28	13.49	228.283
0.902	0.3561	0.787	973.8364	262.60	19242.22	10.52	253.568
0.878	0.3392	0.768	1397.807	368.08	26971.78	15.1	275.070
0.854	0.3227	0.755	1749.573	452.92	33188.4	18.9	284.401
0.843	0.303	0.717	1610.718	395.97	29015.2	17.4	277.847
0.832	0.2865	0.681	1518.148	354.22	25956.07	16.4	271.328

Finite difference treatment

For 1 dimensional treatment of FD, the step employed are:
Calculating T_o for each time period, and T₁ to T₅ using the FD, value of A was

calculated as shown in equation (33). The stencil for the explicit finite difference method for the heat equation of step 3 is given in fig.5

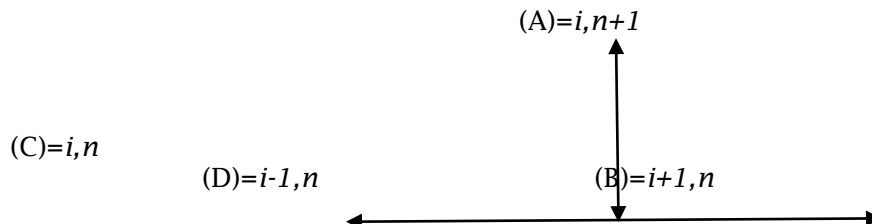


Fig. 5: Stencil for explicit Finite Difference method of heat equation

From fig.5, using the nodal point at (A) =i, n+1, equation 33 is obtained.
 $A = \lambda B + \lambda C + \lambda D$

By substituting the values of A, B, C, and D in equation 33, we have

$$T_{i,n+1} = \lambda T_{i+1,n} + (1 - 2\lambda) T_{i,n} + \lambda T_{i-1,n} \quad (34)$$

Where $\lambda = \frac{\alpha \Delta t}{\Delta x^2}$

For steel of $Mn < 0.1 \leq 0.8\%$ and $Si \leq 0.1\%$;
 α = thermal diffusivity of steel = $1.775 \times 10^{-6} (m^2/s)$ (Theodora L. et al., 2011)

Discretization of temperature development across the thickness

The temperature development across the thickness is shown in fig. 6.

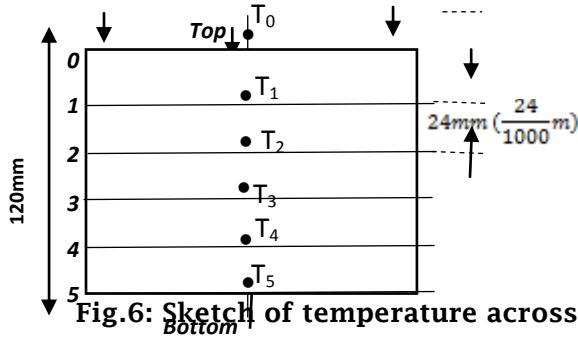


Fig.6: Sketch of temperature across the thickness from top to bottom plate

For the 1 -D “EXPLICIT F.D” to converge to a good solution, the stability is based on the conditions that;
 $\{ 0 < \lambda \leq 1/2 \}$ (Crank, J., 2015)

If α = thermal diffusivity of steel = $1.775 \times 10^{-6} m^2/s$, for $\Delta x = 24/1000$, and $\Delta t = 30$ sec for the interval of each time used. Then solving for λ in equation 34, we have

$$T_{i,n+1} = \lambda T_{i+1,n} + ((1 - 2\lambda) T_{i,n}) + \lambda T_{i-1,n}$$

$$\lambda = \frac{\alpha \Delta t}{\Delta x^2} = \frac{1.775 \times 10^{-6} \times 30}{0.024^2}$$

$$\lambda_{@30 \text{ sec interval}} = \frac{1.775 \times 10^{-6} \times 30}{0.000576} = 0.092$$

The condition for good convergence, therefore becomes
 $\{ 0 < 0.092 \leq 1/2 \}$

Thus, equation 34 becomes

$$T_{i,n+1} = 0.092 T_{i+1,n} + 0.816 T_{i,n} + 0.092 T_{i-1,n} \quad (35)$$

Equation 35 was then simulated using visual Basic Heat Transfer Model programme to determine the temperature distributions across the workpiece. The data obtained were used to plot and analyze the temperature parametric studies on the impingement gaps.

Fig. 7, shows the effect of impingement gaps, $H = 40\text{mm}, 50\text{mm}, 60\text{mm},$ and 70mm at constant pipe diameter, $D = 20\text{mm}$ on temperature - time cooling curve on run-out table. The cooling took place at the surface temperatures of $438^\circ\text{C}, 440^\circ\text{C}, 463^\circ\text{C}$ and 469°C . The steeper curve was an indication of a faster rate of cooling at impingement gap $H = 70\text{mm}$ at constant diameter $D = 20\text{mm}$ that occurred at a controlled temperature of 300°C , where optimum cooling was shown.

Parametric Analysis of Impingement gap on Hot Steel Cooling Using Water Jet at $D = 20\text{mm}$, and $40\text{mm}, 50\text{mm}, 60\text{mm}$ and $H = 70\text{mm}$

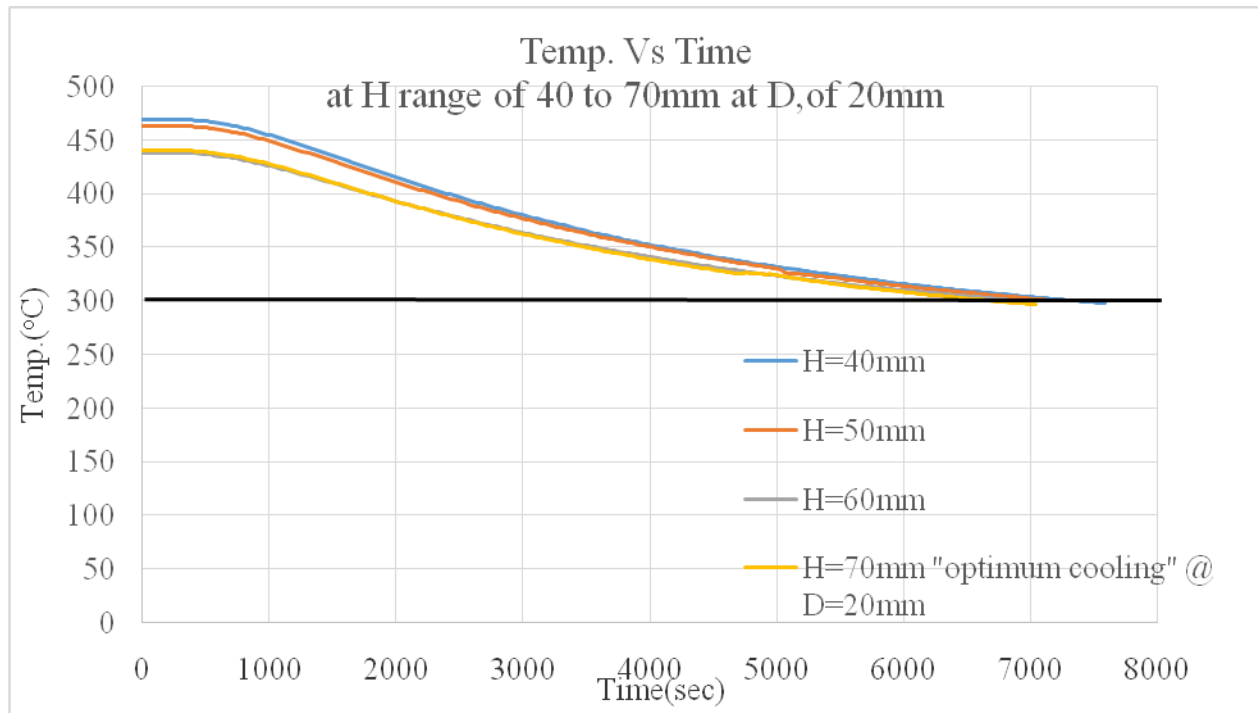


Fig.7:Parametric study of impingement gap on Hot Steel Plate cooling using water jet of D =45mm , and of , H=40mm, 50mm, 60mm and 70mm on temperature - time cooling curve on run-out table

Parametric Analysis of Impingement gap on Hot Steel Plate Cooling Using Water Jet at D=45mm, and H=40mm, 50mm, 60mm, and 70mm

Fig. 8, shows also the effect of impingement gaps ,H = 40mm, 50mm, 60mm, and 70mm at constant pipe diameter D= 45mm on temperature - time cooling curve on run-out table. The cooling took place at the surface temperatures of 458°C, 470°C , 500°C and 500°C respectively. The steeper curve was

an indicative of a faster rate of cooling at impingement gap H=40mm at constant diameter D= 45mm that occurred at a controlled temperature of 300°C, where optimum cooling was indicated.

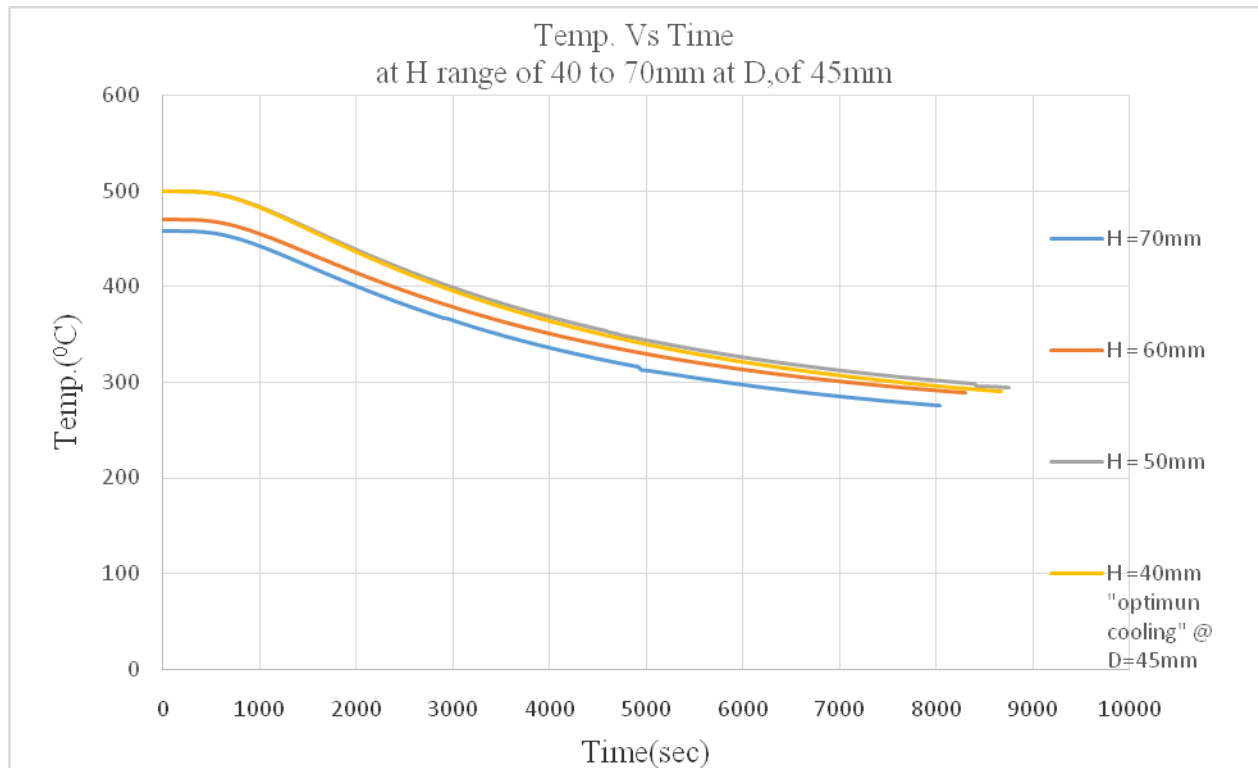


Fig.8 : Parametric study of impingement gap on Hot Steel Plate cooling using water jet of $D = 45\text{mm}$, and of, $H=40\text{mm}$, 50mm , 60mm and 70mm on temperature - time cooling curve on run-out table

CONCLUSION

Parametric analysis of impingement gaps on Hot Steel Plate Cooling by water jet for the pipe diameters, D , of 20mm and 45mm were investigated. The cooling took place at the initial temperatures of 438°C , 440°C , 463°C and 469°C , with pipe diameter, D , of 20mm , and 458°C , 470°C , 500°C and 500°C , with pipe diameter, D , of 45mm . The steeper curves are an indication of a faster rate of cooling at impingement gaps, H , of 70mm and 40mm , and pipe diameters, D , of 20mm and 45mm . Based on the

analysis, it was found that the optimum coolings occurred at small pipe diameter, D , of 20mm and at high impingement gap, H , of 70mm , and also with big pipe diameter, D , of 45mm at impingement gap, H , of 40mm . This parametric study showed that, with the small pipe diameter, the rate of cooling was achieved at high impingement gap, but with big pipe diameter the rate of cooling was better achieved with small diameter pipe [10,11,12,13]

This could be as a result of streamwise velocity [14], that water jet

velocity for planar or water curtain jet does not decrease, whereas water jet velocity in parallel flow zone of circular jets decreases. It was inferred that the cooling of Hot steel plates should be

done with small pipe diameters of high impingement gaps. However, also with big pipe diameter, small impingement gaps should be employed [15, 16, 17].

REFERENCES

1. Bangalore, (2014). *Mathematics textbook*, 10th edition.
2. Cho, C. S. K., and Wu, K., (2015). "Comparison of Burnout Characteristics in Jet Impingement Cooling and Planar Cooling," Proc. National Heat Transfer Conf., Houston, Texas, pp. 561-567.
3. Colas and Sellars, (2013). Modelling of heat transfer during hot rolling of steel strip", Modelling Simul. Mater. Sci. Eng., Vol. 3, No. 4, pp. 437- 453.
4. Grank, J. (2015). *The Mathematics of Diffusion*. 2nd Edition, Oxford, P. 143.
5. Hernandez, V.H. (2011). Modelling of Thermal Evolution on Steel Strips cooled in the rolling Run-out Table, Ph.D Thesis, MMAT, University of British Columbia.
6. Jeffery, A. (2011). *Advanced Engineering Mathematics*, Academic Press.
7. Theodora L., Bergman, Adrienne S., David P., and Dewitt, (2011). *Fundamentals of Heat and Mass Transfer, Seventh Editions*: Thermo physics Properties of Thermal Conductivity of Liquids and Vapours, Table A - 6, by John Wiley & Sons Inc
8. Theodora L., Bergman, Adrienne S., David P., and Dewitt, (2011). *Fundamentals of Heat and Mass Transfer, seventh Edition*, India Edition: Thermo Physics Properties of liquid and Vapour Table A - 4, by John Wiley & Sons Inc.
9. Theodora L., Bergman, Adrienne S., David P., and Dewitt, (2011). *Fundamentals of Heat and Mass Transfer, seventh Edition*: Thermophysics Properties of Selected Metallic Solids Table A - 1, by John Wiley & Sons Inc.
10. Liu, Z.H., and Wang, J. (2014). Study on Film Boiling Heat Transfer for Water Jet Impinging on High Temperature Flat Plate, *Int.J. Heat Mass Transfer*, 44:2475 - 2481.
11. Prodanovic, V., Fraser, D., and Mihtzer, M. (2014). Simulation of Run-out Table Cooling by Water Jet Impingement on Stationary Plates - A novel experimental Method, 2nd International Conference on Thermochemical processing of Steel Ed. M. Lamberights, Liege, Belgium, 25-320.
12. Pyykkonen, Hamed, M. S., Shoukri, M (2015). The cooling of a hot steel plate by an impingement water jet
13. Sergners, J. V., and Watons, T. T. R. (2015). *Journals of Physical, and Chemicals Reference Data for Viscosity and thermal Conductivity*, Table A - 9.
14. Sengers, J. S., and Watson, T. T. R. (2015). *Journals of Physical and Chemical Reference Data, Properties of Temperature and Prandtl Nu.*, Tables A - 9 Appendix I.

15. Timm W., Weinzierl, K. and Leipertz, A. (2010). Heat Transfer in Subcooled Jet Impingement Boiling at High Wall Temperatures, *Int. J. of Heat and Mass Transfer*, Vol. 46, pp. 1385- 1393,
16. Webb, B.W., Ma C.F. (2015). Single-Phase liquid Jet Impingement Heat Transfer. *In. J.P. Hartnett. Advances in Heat Transfer* . Vol.26, Academic Press, New York. PP.105- 215,
17. Wolf, D. H., Incropera, F. P., Viskanta, R. (2013). *Advances in Heat Transfer*, 23:1-131.